Isoscalar monopole and quadrupole modes in Mo isotopes: Microscopic analysis

Gianluca Colò [a,b,∗], Danilo Gambacurta [c,d], Wolfgang Kleinig [e], Jan Kvasil [f], Valentin O. Nesterenko [e,g,h], Alessandro Pastore [i]

[a] *Dipartimento di Fisica "Aldo Pontremoli", Università degli Studi di Milano, via Celoria 16, I-20133 Milano, Italy*
[b] *INFN, Sezione di Milano, Via Celoria 16, I-20133 Milano, Italy*
[c] *Extreme Light Infrastructure - Nuclear Physics (ELI-NP), Horia Hulubei National Institute for Physics and Nuclear Engineering, 30 Reactorului Street, RO-077125 Magurele, Jud. Ilfov, Romania*
[d] *LNS-INFN, I-95123, Catania, Italy*
[e] *Laboratory of Theoretical Physics, Joint Institute for Nuclear Research, Dubna, Moscow Region, 141980, Russia*
[f] *Institute of Particle and Nuclear Physics, Charles University, CZ-18000, Praha 8, Czech Republic*
[g] *State University "Dubna", Dubna, Moscow Region, 141980, Russia*
[h] *Moscow Institute of Physics and Technology, Dolgoprudny, Moscow Region, 141701, Russia*
[i] *Department of Physics, University of York, Heslington, York, YO10 5DD, UK*

A B S T R A C T

The recent RCNP (α, α') data on the Isoscalar Giant Monopole Resonance (ISGMR) and Isoscalar Giant Quadrupole Resonance (ISGQR) in ^{92,94,96,98,100}Mo are analyzed within a fully self-consistent Quasiparticle Random Phase Approximation (QRPA) approach with Skyrme interactions, in which pairing correlations and possible axial deformations are taken into account. The Skyrme sets SkM*, SLy6, SVbas and SkP$^\delta$, that explore a diversity of nuclear matter properties, are used. We discuss the connection between the line shape of the monopole strength ISGMR and the deformation-induced coupling between the ISGMR and the $K = 0$ branch of the ISGQR. The ISGMR is best described by the force SkP$^\delta$, having a low incompressibility $K_\infty = 202$ MeV. The ISGQR data are better reproduced by SVbas, that has large isoscalar effective mass $m^*/m = 0.9$. The need of a functional that can describe simultaneously the ISGMR and ISGQR data is stressed, with the requirement of suitable values of K_∞ and m^*/m. Possible extensions of the QRPA to deal with soft systems are also envisaged.

1. Introduction

There is still a high theoretical and experimental interest in the determination of the parameters of the Equation of State (EoS) of nuclear matter (NM) [1]. Among these parameters, the nuclear incompressibility K_∞ and the isoscalar effective mass m^*/m constitute crucial benchmarks for testing new models and provide an indispensable guideline for applications of nuclear theory to heavy-ion collisions [2], astrophysical processes [3,4], and other areas.

The incompressibility of symmetric NM (SNM) is defined as

$$K_\infty = 9\rho_0^2 \frac{d^2}{d\rho^2}\left(\frac{E}{A}\right)_{\rho=\rho_0}, \qquad (1)$$

where E/A is the energy per particle and ρ_0 is the saturation density at which the EoS displays a minimum ($\rho_0 = 0.16$ fm^{-3}). Being related to the second derivative of the EoS around this minimum, K_∞ measures the stiffness of SNM with respect to the compression. It can be linked to compressional modes of finite nuclei, in particular to the isoscalar giant monopole resonance (ISGMR), a breathing mode characterised by a strong transition amplitude from the ground-state [5,6]. Indeed the ISGMR is the main, although indirect, source of information on K_∞.

The discussion on how to extract K_∞ from the ISGMR dates back to the years 1980s [5] (for the present state-of-the-art, cf. the recent review [6]). Nowadays, there is a general consensus that the relationship between the ISGMR energy and K_∞ may be only obtained within the self-consistent Energy Density Functional (EDF)

* Corresponding author.
E-mail addresses: colo@mi.infn.it (G. Colò), gambacurta@lns.infn.it (D. Gambacurta), kleinig@theor.jinr.ru (W. Kleinig), kvasil@ipnp.troja.mff.cuni.cz (J. Kvasil), nester@theor.jinr.ru (V.O. Nesterenko), alessandro.pastore@york.ac.uk (A. Pastore).
URL: http://www.mi.infn.it/~colo (G. Colò).

theory [7,8]. As shown by various EDF calculations, in nuclei like ^{90}Zr or ^{208}Pb the computed ISGMR energy correlates well with the value of K_∞ of the given functional. This allows, at least in principle, to consider as correct the K_∞ value associated with the EDF which reproduces the ISGMR experimental data.

However, the exploration of ISGMRs and their relation to K_∞ still has some unresolved problems. While K_∞ extracted from ^{208}Pb is around 240 ± 20 MeV, its value in Sn and other open-shell nuclei is lower by $\approx 10\%$ i.e. open-shell nuclei show up some softness against the compression, see e.g. [9–11]. This can be partly explained by pairing correlations in open-shell nuclei, which somewhat shift the ISGMR towards lower energies due to the attractive character of the pairing force [10]. However, the quantitative results depend to some extent on the choice of the parameters of that force [11]. So this problem, often referred to as "why open-shell nuclei are soft", still remains open.

ISGMR in deformed nuclei deserves a special attention. When a nucleus displays an axial deformation in its intrinsic frame, the total angular momentum J is no longer a good quantum number and the nuclear states are characterised by the projection K of the angular momentum on the intrinsic symmetry axis. If the reflection symmetry is kept, such states are superpositions of contributions from different J and the same parity. In particular, $K = 0$ monopole states are coupled to $K = 0$ quadrupole (hexadecapole, etc.) states, which can lead to an appreciable mixing of the ISGMR and $K = 0$ ISGQR. Then, the monopole strength is redistributed and, in addition to the main ISGMR, there appears a minor low-energy monopole branch at the same energy as the $K = 0$ ISGQR branch. This is the deformation-induced splitting of the ISGMR.

Following early macroscopic models [12–14], and a recent self-consistent Skyrme Quasiparticle Random Phase Approximation (QRPA) [15] analysis, the ISGMR/ISGQR mixing is not complete and still preserves the main character of each resonance. In addition, the deformation can shift the energy of the main ISGMR peak (upward in prolate nuclei and downward in oblate nuclei) [12–15]. This deformation effect, being distinctive in well-deformed nuclei, becomes more subtle in nuclei with moderate deformation (i.e., for $\beta < 0.2$, where β is the quadrupole deformation parameter) [15]. A further microscopic study of this point is desirable, e.g. like that for Nd and Sm isotopes in Ref. [16] (see also Ref. [17] where the monopole in Sm isotopes is calculated using a relativistic mean-field approach). Such study obviously calls for EDFs that reproduce equally well the monopole and quadrupole strengths. While the ISGMR peak energy correlates with K_∞, the ISGQR energy is sensitive to the nucleon isoscalar effective mass m^*/m [5,18]. The values K_∞ and m^*/m are coupled in SNM, at least for Skyrme EDFs with $m^*/m \neq 1$ [19]. This is an additional argument to consider the ISGMR and ISGQR simultaneously.

Inelastic α-scattering data for ^{92,94,96,98,100}Mo at incident laboratory energy $E_\alpha = 386$ MeV have been recently obtained at RCNP [20,21]. These data supplement the previous experimental results for Mo isotopes from TAMU [22,23] and for ^{92}Mo from RCNP [24,25]. Soft Mo isotopes seem to be ideal candidates to discuss the open questions introduced above.

It has to be noted that, in the present RCNP [20] and earlier TAMU [22,23] experiments, different prescriptions to analyse the experimental data are employed. The comparison between the methodologies of these two groups is discussed in [6]. TAMU data for giant resonances usually display a significant high-energy tail, while RCNP data, including those from [20], do not. This difference affects the extracted values of ISGMR energy centroids. To exclude this ambiguity, we do not use in our analysis the energy centroids but rather the overall shape of the strength distributions with their peak energies. In this regard, note that RCNP and TAMU data give close ISGMR peak energies (see, e.g., the results for ^{92}Mo in Fig. 3 of the present study and in Fig. 4 of Ref. [22]).

Table 1
Incompressibility K_∞ and isoscalar effective mass m^*/m for the Skyrme forces SVbas, SLy6, SkM*, and SkP$^\delta$.

	SVbas	SLy6	SkM*	SkP$^\delta$
K_∞ [MeV]	234	230	217	202
m^*/m	0.9	0.69	0.79	1

In this study, we analyze the Mo data within fully self-consistent Skyrme QRPA models. In Ref. [20], these data have been presented in conjunction with simple RPA calculations that do not account for the existence of pairing and possible deformation in the Mo isotopes (with the associated monopole-quadrupole coupling). Consequently, here we address the two questions: (i) how do pairing and deformation shape the ISGMR and ISGQR strengths in soft medium-mass deformed nuclei; (ii) how does this impact on our understanding of nuclear incompressibility and isoscalar effective mass.

2. Formalism

The calculations are performed using two different QRPA methods based on Skyrme EDFs. Both methods are fully self-consistent, i.e. their mean field and residual interaction are derived from the initial functionals without approximations. Reflection and axial symmetries are assumed. The agreement between results of these two methods strengthens our conclusions.

We employ a representative set of Skyrme forces (SkM* [26], SLy6 [27], SVbas [28] and SkP$^\delta$ [29]) that span different values of K_∞ and m^*/m (see Table 1). The force SkP$^\delta$ may produce instabilities [30] but it is employed to include the case of low K_∞ and large m^*/m. Giant resonances are less sensitive to such instabilities, although these may show up when the basis size is increased [31].

The first method, called here as QRPA-I, is introduced in Refs. [32,33]. In this method, the nuclear mean field and pairing field are computed with the code SKYAX [34] using a two-dimensional mesh in cylindrical coordinates. In our particular case, the box in which the nuclei are confined extends up to three times the nuclear radii, and the mesh size is 0.4 fm. Pairing correlations are included at the level of the iterative HF-BCS (Hartree-Fock plus Bardeen-Cooper-Schrieffer) method [32]. We use volume pairing for SkM*, SLy6, and SkP$^\delta$, and density-dependent pairing for SVbas. The proton and neutron pairing strengths are fitted to reproduce empirical pairing gaps obtained from the five-point formula along selected isotopic and isotonic chains [28]. To cope with the divergent character of zero-range pairing forces, energy-dependent cut-off factors are used. QRPA is implemented in the matrix form. The two-quasiparticle (2qp) configuration space extends up to 80 MeV, which allows to exhaust the isoscalar E0 and E2 energy-weighted sum rules. The pairing-induced spurious admixtures are extracted following the prescription of [35].

The second method, called as QRPA-II, follows closely Ref. [36]. The Hartree-Fock-Bogoliubov (HFB) equations are solved in an axially deformed harmonic oscillator (HO) basis by using the code HFTHO [37]. A canonical basis with 14 major HO shells is used. As additional cut-off, canonical states with energies larger than 200 MeV or pairs with occupation factors $v^2 < v^2_{\text{crit}} = 10^{-2}$ are discarded. For each Skyrme force, the pairing strength is fixed so that the canonical neutron pairing gap $\Delta_n = 1.4$ MeV in ^{120}Sn is reproduced. QRPA eigenvalues and eigenvectors are found by using diagonalization techniques for sparse matrices.

The implementation of various prescriptions in the cases I and II allows us to conclude that: (i) the inclusion of pairing is mandatory, and (ii) the details of the procedure (HFB vs. HF-BCS) or of the pairing force are not crucial, as far as the resulting pairing gaps
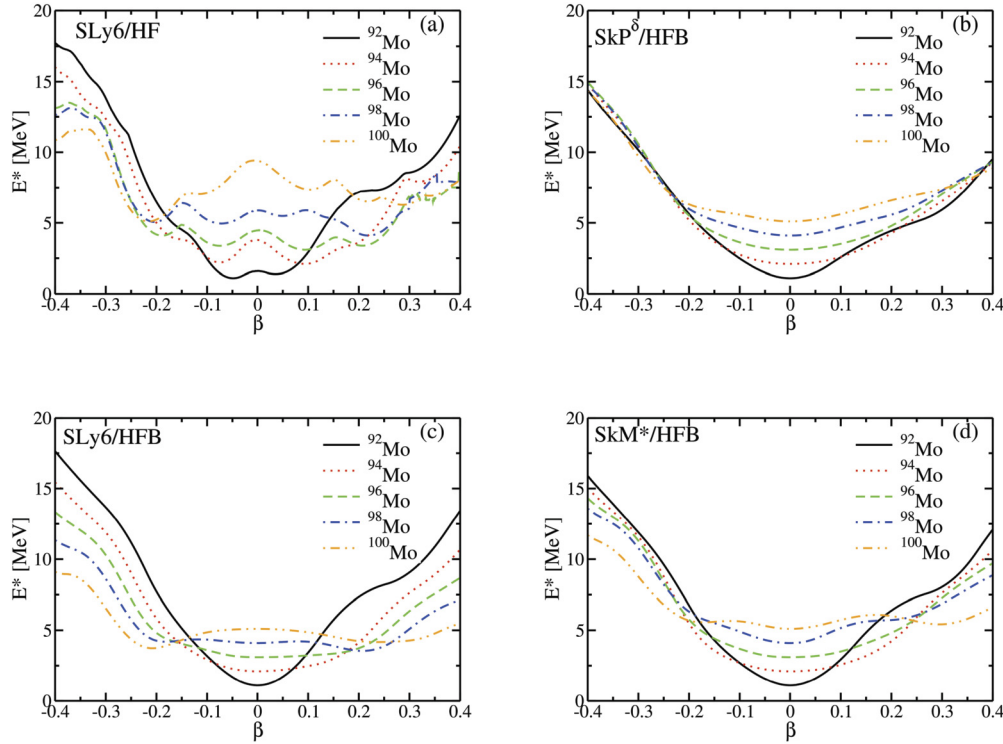
Fig. 1. Potential energy curves obtained by constrained calculations with different Skyrme forces. In the left panels, we report results obtained with SLy6 at the level of HF (upper panel) and HFB (lower panel). In the upper right (lower right) panels, HFB results associated with the SkP$^\delta$ (SkM*) functional are displayed.

are close to the empirical ones. In fact, all our models lead to similar results in the Mo isotopes: proton gaps are slightly larger than neutron gaps but all are around 1 MeV. Fine details will be reported elsewhere.

3. Results for the Mo isotopes

3.1. Ground-state deformation and softness

In this subsection we discuss the calculated potential energy curves (PECs) for various Skyrme EDFs. Though some Mo isotopes may exhibit triaxiality [38], we restrict ourselves, for the sake of simplicity, to the case of axial deformation characterised by the deformation parameter β. Each PEC point is obtained by minimization of the total ground-state energy under the constraint of a fixed β (and corresponding quadrupole moment).

In Fig. 1 we display the PECs obtained by our method II for SkM*, SLy6, and SkP$^\delta$. The comparison of SLy6 results obtained by HF (upper left panel) and HFB (lower left panel) shows that pairing has the important effect of smoothing the PECs. This can be probably attributed to the fact that pairing correlations smear out the occupancies and so make the total energies less sensitive to details of the deformed single-particle levels.

Fig. 1 shows that PECs associated with different EDFs, albeit not identical, lead to the same qualitative outcome. Pairing makes the spherical minima more favoured but, overall, Mo isotopes look soft against quadrupole deformation. The softness increases with the neutron number. Even in ^{92}Mo the potential is not steep although the spherical minimum is well defined. In the heavier isotopes, the potential is increasingly shallow and the spherical minimum is not well defined at all. The extreme case of a flat potential is reached for ^{98}Mo and ^{100}Mo. In the case of SLy6, ^{100}Mo displays even a kind of convex potential. We do not plot PECs for SVbas, but we have checked that they are consistent with all the above conclusions.

It is not easy to obtain a straight experimental confirmation of ground-state (g.s.) deformation in soft nuclei. The isotopes ^{94,96,100}Mo exhibit g.s. rotational bands with $J^\pi = 0^+, 2^+, 4^+, 6^+, 8^+$ [39], and so they should have at least a modest axial quadrupole deformation. The values of the deformation parameter, extracted from E2 transitions in the g.s. band, are $\tilde{\beta} = 0.109, 0.151, 0.172, 0.168, 0.162$ for A = 92, 94, 96, 98, 100, respectively [39]. However, in soft nuclei, the deformation parameters obtained in such a way can be overestimated. This is confirmed by the fact that the energies of the first 2^+ states in ^{94,96,98}Mo, calculated with $\tilde{\beta}$, are lower than the experimental values. In summary, the values $\tilde{\beta}$ should be rather considered as upper limits of the true deformation parameters.

In keeping with all these facts, we performed QRPA calculations for the Mo isotopes both on top of the self-consistent minimum (which is spherical in most of the cases), and with the constraint $\beta = \tilde{\beta}$. This provides us a proxy for the softness and theoretical uncertainties in our quest on how the strengths are sensitive to a modest axial deformation.

3.2. QRPA strength distributions

In this subsection we discuss our main results, namely, QRPA strength distributions. The isoscalar monopole (L = 0) and quadrupole (L = 2) strengths are defined in the usual way as

$$S_L(E) = \sum_{K=0}^{L} (2 - \delta_{K,0}) \sum_{\nu \in K} |\langle \nu | \hat{O}_{LK} | 0 \rangle|^2 \xi_\Delta(E - E_\nu), \qquad (2)$$

where ν labels the complete set of QRPA eigenvalues $|\nu\rangle$ with the energies E_ν, $|0\rangle$ is QRPA ground-state, and the monopole and quadrupole isoscalar transition operators read $\hat{O}_{00} = \sum_i^A r_i^2 Y_{00}(\hat{r}_i)$ and $\hat{O}_{2K} = \sum_i^A r_i^2 Y_{2K}(\hat{r}_i)$. For a more convenient comparison with experimental data, the strength is smoothed by the Lorentz weight $\xi_\Delta(E - E_\nu) = \Delta/(2\pi[(E - E_\nu)^2 - \Delta^2/4])$, with the averaging parameter $\Delta = 2.5$ MeV.
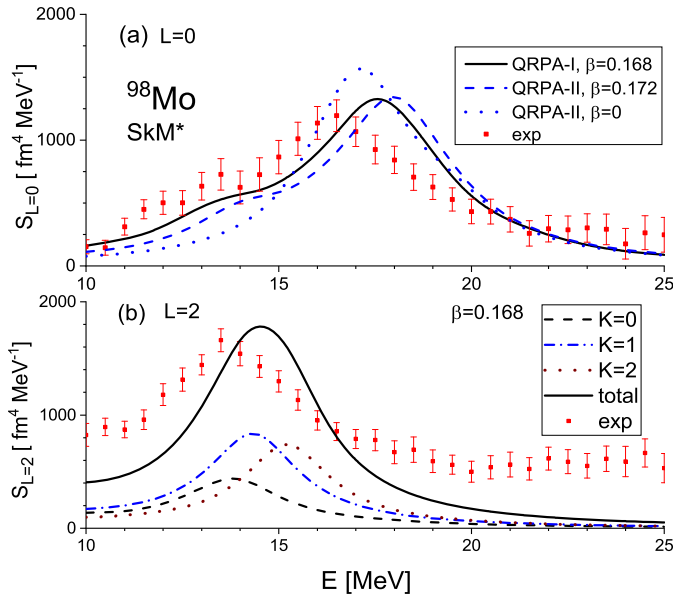
Fig. 2. a) Monopole ($L = 0$) strengths in ^{98}Mo, calculated within QRPA-I and QRPA-II. b) Quadrupole ($L = 2$) strengths in ^{98}Mo, calculated within QRPA-I. In both panels, the experimental data from [20,21] are used.

Before a general discussion of ISGMR and ISGQR along the Mo isotope chain, we would like to highlight some important points. They are illustrated in Fig. 2 for the SkM* strengths in ^{98}Mo.

1) In panel (a), the monopole strengths obtained by QRPA-I and QRPA-II at close deformations $\beta = 0.168$ and 0.172 are compared. Though the implementations are slightly different, the QRPA-I and QRPA-II curves are pretty consistent with each other. The slightly higher ISGMR peak energy in QRPA-II can be partly explained by the larger deformation.

2) By comparing in panel (a) two QRPA-II results with different g.s. deformations ($\beta = 0$ and 0.172), we clearly see that even a modest deformation can significantly shift upward the ISGMR peak energy, by $\approx$0.8 MeV in this case. Moreover, the ISGMR has a single peak in the spherical case ($\beta = 0$), and it acquires a noticeable low-energy shoulder at deformation $\beta = 0.172$.

3) In panel (b), the deformation splitting of the ISGQR into branches with $K = 0, 1, 2$ is shown. It is easy to see that the IS-GMR shoulder of QRPA-I in panel (a) and the $K = 0$ branch of the ISGQR in panel (b) lie in the same energy interval. This confirms that the shoulder arises due to the deformation-induced coupling of the monopole and quadrupole modes.

From Fig. 2, we also note that SkM* significantly overestimates both ISGMR and ISGQR experimental peak energies. This indicates that the values $K_\infty = 217$ MeV and $m^*/m = 0.79$ are not optimal. For a better reproduction of the experimental data, smaller (larger) values of K_∞ (m^*/m) are desirable.

In Fig. 3, we provide a general view on monopole and quadrupole strength along the isotopic chain. QRPA-I results obtained with different Skyrme forces at the deformations $\beta = \tilde{\beta}$ (see above) are compared with the experimental data [20,21]. The data show that, in addition to the main ISGMR peak, a low-energy shoulder appears in ^{94,96,98}Mo. This structure resembles more a double hump in ^{100}Mo. The larger the deformation of the isotope, the more pronounced the shoulder. As discussed in connection with Fig. 2, the shoulder is caused by the deformation-induced monopole-quadrupole coupling. So one may conclude that this coupling can manifest itself even at modest deformations, $\beta = 0.15$-0.18.

Fig. 3 shows that SVbas ($K_\infty = 234$ MeV), SLy6 ($K_\infty = 230$ MeV), and SkM*($K_\infty = 217$ MeV) overestimate the experimental ISGMR

peak energies by 1.4-2.8 MeV, 1.0-2.2 MeV and 0.6-1.8 MeV, respectively. For all these three forces, the overestimate is minimal in ^{92}Mo and maximal in ^{94}Mo. SkP$^\delta$ ($K_\infty = 202$ MeV) reproduces the ISGMR data much better: the overestimate of the peak energies are 0.0 MeV (^{92}Mo), 0.8 MeV (^{94}Mo), 0.5 MeV (^{96}Mo), 0.2 MeV (^{98}Mo), and 0.1 MeV (^{100}Mo). Thus Mo isotopes call for a quite low value of K_∞. However, the strong effect of the monopole-quadrupole coupling prevents us from a quantitative conclusion on the value of K_∞.

Moving to the quadrupole strengths in Fig. 3, we first of all notice that the experimental data of [21] do not show fine structures in all isotopes, aside from ^{96}Mo (that has the largest $\tilde{\beta}$). As discussed in Ref. [40], deformation mainly produces a broadening of the ISGQR. This is confirmed by Fig. 2, where the splitting of the ISGQR into K-components is shown to be too small to distinguish the separate K-branches in the total strength distribution.

As already mentioned, the ISGQR peak energy correlates with the effective mass m^*/m [18] or, more precisely, with $\sqrt{m^*/m}$ [5]. From Fig. 3, SLy6 and SkM* with their low effective masses (0.79 and 0.69, respectively) significantly overestimate the ISGQR peak energy. Instead, SkP$^\delta$ with $m^*/m = 1$ systematically underestimate it. SVbas with $m^*/m = 0.9$ gives the best agreement: its ISGQR peak energies overestimate the experimental data only by 0.1-0.5 MeV. In Ref. [18], it has been noted that a larger value of the effective mass, $m^*/m > 0.9$, would spoil the description of the isovector GDR. So a value of $m^*/m \approx 0.9$ seems to be optimal.

It is interesting to note that, within the standard Skyrme framework, there is an implicit relationship between ISGMR and ISGQR. In fact, in the Skyrme EoS for SNM, K_∞ and m^*/m are expressed as [19]

$$K_\infty = B + C\sigma + D(1 - \frac{3}{2}\sigma)\Theta, \quad \frac{m^*}{m} = [1 + \frac{m\rho_0}{8\hbar^2}\Theta]^{-1}, \qquad (3)$$

where B, C, and D are simple functions of the saturation density ρ_0 and saturation energy of SNM, σ is the power in the density-dependent t_3-term of the Skyrme force, and Θ is a simple combination of Skyrme parameters related to momentum-dependence. Following Eq. (3), K_∞ and m^*/m are correlated if Θ is not zero (that is, if $m^*/m \neq 1$). Then, the simultaneous description of the ISGMR and ISGQR is desirable to provide tight constraints on the Skyrme parameters. Note that other families of EDFs may not display such a clear correlation between K_∞ and m^*/m.

4. Conclusions and perspectives

New data on monopole and quadrupole strength distributions in ^{92,94,96,98,100}Mo have been obtained in a recent α-inelastic scattering experiment at RCNP, Osaka [20,21]. The main purpose of this paper is the description of these data within state-of-the-art Quasiparticle Random Phase Approximation (QRPA) methods with Skyrme interactions. To this aim, a relevant set of Skyrme forces (SkM* [26], SLy6 [27], SVbas [28] and SkP$^\delta$ [29]), characterised by different values of incompressibility K_∞ and isoscalar effective mass m^*/m, is selected.

We show that, in the ground state (g.s.), both the inclusion of pairing and the breaking of spherical symmetry play important roles. With pairing, different EDFs give similar predictions. In particular, we demonstrate that: (i) Mo isotopes are generally soft with respect to quadrupole deformation, and (ii) this softness increases with the mass number. In the most neutron-rich Mo isotopes, the potential energy curve (PEC) as a function of the deformation parameter β looks very shallow. Pairing has the important effect of smoothing out PECs.

Our QRPA calculations based on a slightly deformed g.s. reproduce the shape of the monopole strength distributions. In
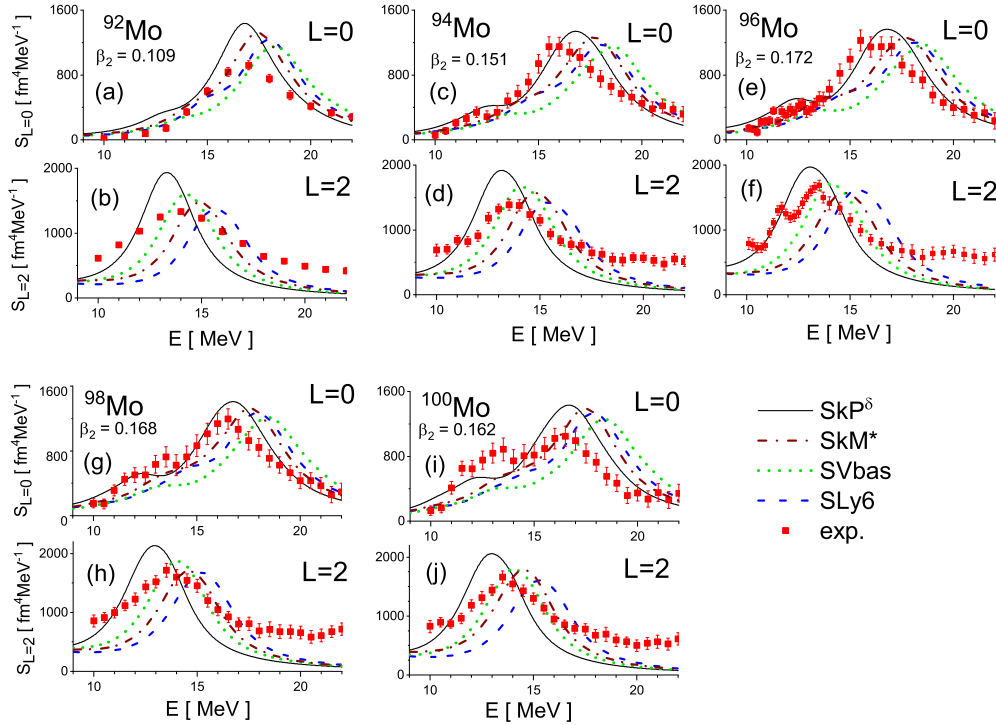
Fig. 3. Isoscalar monopole (L = 0) and quadrupole (L = 2) strengths in ^{92,94,96,98,100}Mo, calculated in the framework of QRPA-I with the Skyrme forces SkM*, SLy6, SVbas and SkP$^\delta$. The strengths are compared with the experimental data [20,21].

^{94,96,98,100}Mo, the monopole strength displays a main peak and lower-energy shoulder. Following our analysis, this shoulder is produced by the deformation-induced coupling of ISGMR and ISGQR. So, even in nuclei with a modest deformation (β = 0.15-0.18 in our calculations) this coupling can have a visible effect.

It is also shown that Skyrme forces with K_∞ between 217 and 234 MeV significantly overestimate the ISGMR peak energies, while SkP$^\delta$ with $K_\infty = 202$ MeV gives acceptable results that lie much closer to the data. For the successful description of the ISGQR in Mo isotopes, we need Skyrme forces with $m^*/m \approx 0.9$ like SVbas and, to a lesser extent, SkP$^\delta$. In general, it is desirable that ISGMR and ISGQR are described consistently, but this is even more true in deformed nuclei where these two resonances are coupled.

The conclusion from our calculations that K_∞ should be smaller than 210 MeV and $m^*/m \approx 0.9$ should be taken with reasonable care in keeping, also, with the limitations of existing EDFs that we have discussed. Moreover, QRPA is not a reliable theory for soft nuclei. To solve this issue, theories that account properly for shape coexistence like multi-reference DFT (see [41] and Refs. therein) are an option. However, so far, they have been applied to low-lying spectroscopy but not to giant resonances in nuclei with a flat PEC. Therefore, Mo isotopes themselves and the extraction of EoS parameters therefrom, deserve in future a more careful analysis. At the same time, remaining discrepancies between the RCNP and TAMU experimental data should be definitely clarified.

Declaration of competing interest

The authors declare that they have no known competing financial interests or personal relationships that could have appeared to influence the work reported in this paper.

Acknowledgements

References

[1] X. Roca-Maza, N. Paar, Prog. Part. Nucl. Phys. 101 (2018) 96.
[2] G. Giuliani, H. Zheng, A. Bonasera, Prog. Part. Nucl. Phys. 76 (2014) 116.
[3] S.E. Woosley, A. Heger, T.A. Weaver, Rev. Mod. Phys. 74 (2002) 1015.
[4] A. Burrows, D. Vartanyan, J.C. Dolence, M.A. Skinner, D. Radice, Space Sci. Rev. 214 (2018) 33.
[5] J.P. Blaizot, Phys. Rep. 64 (1980) 171.
[6] U. Garg, G. Colò, Prog. Part. Nucl. Phys. 101 (2018) 55.
[7] N. Schunck (Ed.), Energy Density Functional Methods for Atomic Nuclei, IoP Publishing, 2019.
[8] G. Colò, Adv. Phys. X 5 (2020) 1740061.
[9] P. Avogadro, C.A. Bertulani, Phys. Rev. C 88 (2013) 044319.
[10] J. Li, G. Colò, J. Meng, Phys. Rev. C 78 (2008) 064304.
[11] E. Khan, J. Margueron, G. Colò, K. Hagino, H. Sagawa, Phys. Rev. C 82 (2010) 024322.
[12] Y. Abgrall, B. Morand, E. Caurier, B. Grammaticos, Nucl. Phys. A 346 (1980) 431.
[13] S. Jang, Nucl. Phys. A 401 (1983) 303.
[14] S. Nishizaki, K. Andō, Prog. Theor. Phys. 73 (1985) 889.
[15] J. Kvasil, V.O. Nesterenko, A. Repko, W. Kleinig, P.-G. Reinhard, Phys. Rev. C 94 (2016) 064302.
[16] K. Yoshida, T. Nakatsukasa, Phys. Rev. C 88 (2013) 034309.
[17] T. Nikšić, N. Kralj, T. Tutiš, D. Vretenar, P. Ring, Phys. Rev. C 88 (2013) 044327.
[18] V.O. Nesterenko, W. Kleinig, J. Kvasil, P. Vesely, P.-G. Reinhard, Int. J. Mod. Phys. E 17 (2008) 89.
[19] E. Chabanat, P. Bonche, P. Haensel, J. Meyer, R. Schaeffer, Nucl. Phys. A 627 (1997) 710.

[20] K. Howard, U. Garg, M. Itoh, H. Akimune, M. Fujiwara, T. Furuno, Y. Gupta, M. Harakeh, K. Inaba, Y. Ishibashi, K. Karasudani, T. Kawabata, A. Kohda, Y. Matsuda, M. Murata, S. Nakamura, J. Okamoto, S. Ota, J. Piekarewicz, A. Sakaue, M. Şenyiğit, M. Tsumura, Y. Yang, Phys. Lett. B 807 (2020) 135608.

[21] K. Howard, arXiv:2004.02362v1 [nucl-exp], 2020.

[22] D.H. Youngblood, Y.-W. Lui, Krishichayan, J. Button, M.R. Anders, M.L. Gorelik, M.H. Urin, S. Shlomo, Phys. Rev. C 88 (2013) 021301.

[23] D.H. Youngblood, Y.-W. Lui, Krishichayan, J. Button, G. Bonasera, S. Shlomo, Phys. Rev. C 92 (2015) 014318.

[24] Y. Gupta, U. Garg, K. Howard, J. Matta, M. Şenyiğit, M. Itoh, S. Ando, T. Aoki, A. Uchiyama, S. Adachi, M. Fujiwara, C. Iwamoto, A. Tamii, H. Akimune, C. Kadono, Y. Matsuda, T. Nakahara, T. Furuno, T. Kawabata, M. Tsumura, M. Harakeh, N. Kalantar-Nayestanaki, Phys. Lett. B 760 (2016) 482.

[25] Y.K. Gupta, K.B. Howard, U. Garg, J.T. Matta, M. Şenyiğit, M. Itoh, S. Ando, T. Aoki, A. Uchiyama, S. Adachi, M. Fujiwara, C. Iwamoto, A. Tamii, H. Akimune, C. Kadono, Y. Matsuda, T. Nakahara, T. Furuno, T. Kawabata, M. Tsumura, M.N. Harakeh, N. Kalantar-Nayestanaki, Phys. Rev. C 97 (2018) 064323.

[26] J. Bartel, P. Quentin, M. Brack, C. Guet, H.-B. Håkansson, Nucl. Phys. A 386 (1982) 79.

[27] E. Chabanat, P. Bonche, P. Haensel, J. Meyer, R. Schaeffer, Nucl. Phys. A 635 (1998) 231.

[28] P. Klüpfel, P.-G. Reinhard, T.J. Bürvenich, J.A. Maruhn, Phys. Rev. C 79 (2009) 034310.

[29] J. Dobaczewski, W. Nazarewicz, T.R. Werner, Phys. Scr. T 56 (1995) 15.

[30] V. Hellemans, A. Pastore, T. Duguet, K. Bennaceur, D. Davesne, J. Meyer, M. Bender, P.-H. Heenen, Phys. Rev. C 88 (2013) 064323.

[31] A. Pastore, D. Tarpanov, D. Davesne, J. Navarro, Phys. Rev. C 92 (2015) 024305.

[32] A. Repko, J. Kvasil, V.O. Nesterenko, P.-G. Reinhard, Eur. Phys. J. A 53 (2017) 221.

[33] A. Repko, J. Kvasil, V.O. Nesterenko, P.G. Reinhard, arXiv:1510.01248, 2015.

[34] P.G. Reinhard, Skyax code, unpublished.

[35] A. Repko, J. Kvasil, V.O. Nesterenko, Phys. Rev. C 99 (2019) 044307.

[36] C. Losa, A. Pastore, T. Døssing, E. Vigezzi, R.A. Broglia, Phys. Rev. C 81 (2010) 064307.

[37] M. Stoitsov, J. Dobaczewski, W. Nazarewicz, P. Ring, Comput. Phys. Commun. 167 (2005) 43.

[38] F. Dönau, G. Rusev, R. Schwengner, A.R. Junghans, K.D. Schilling, A. Wagner, Phys. Rev. C 76 (2007) 014317.

[39] National Nuclear Data Center, http://www.nndc.bnl.gov.

[40] C. Kureba, Z. Buthelezi, J. Carter, G. Cooper, R. Fearick, S. Förtsch, M. Jingo, W. Kleinig, A. Krugmann, A. Krumbolz, J. Kvasil, J. Mabiala, J. Mira, V.O. Nesterenko, P. von Neumann-Cosel, R. Neveling, P. Papka, P.-G. Reinhard, A. Richter, E. Sideras-Haddad, F. Smit, G. Steyn, J. Swartz, A. Tamii, I. Usman, Phys. Lett. B 779 (2018) 269.

[41] M. Bender, N. Schunck, J.-P. Ebran, T. Duguet, Single-reference and multi-reference formulations, in: Energy Density Functional Methods for Atomic Nuclei, 2053-2563, IOP Publishing, 2019, p. 3-1.